24. A. Berger, *Quat. Res.* **9**, 139 (1978); A. Berger, J. Imbrie, J. Hays, G. Kukla, B. Saltzman, Eds., *Milankovitch and Climate: Understanding the Response to Astronomical Forcing* (Reidel, Dortrecht, 1984).
25. J. Imbrie and J. Z. Imbrie, *Science* **207**, 943 (1980); J. Imbrie, *J. Geol. Soc. London* **142**, 417 (1985). Evidence for a periodicity of 400,000 years has been observed in Cretaceous shales [T. Herbert and A. Fischer, *Nature* **321**, 739 (1986)] and in deep-sea sediments in the Indian Ocean [ODP Leg 117 Shipboard Scientific Party, *ibid.* **331**, 663 (1988)].
26. Measurements of river water worldwide indicate that average modern runoff has a high $^{87}Sr/^{86}Sr$ ratio (R_r) of about 0.711 and provides a flux (J_r) of 3.0×10^{10} mol of Sr per year to the oceans; the average value of R_r from (*27*) is 0.7102, and the average R_r from M. Palmer and J. Edmond [*Earth Planet. Sci. Lett.* **92**, 11 (1989)] is 0.7119. We choose a value of 0.7110; if a different value were used it would change the details but not the main features of our models.
27. S. Goldstein and S. Jacobsen, *Chem. Geol.* **66**, 245 (1987).
28. Hydrothermal alteration and weathering of oceanic crust contributes Sr with a low $^{87}Sr/^{86}Sr$ ratio (0.7025 to 0.7055); see S. Hart, A. Erlank, F. Kable, *Contrib. Mineral. Petrol.* **44**, 219 (1974); E. Spooner, *Earth Planet. Sci. Lett.* **31**, 167 (1976); F. Albarède, A. Michard, J. Minster, G. Michard, *ibid.* **55**, 229 (1981). Because of the complexity of the exchange process, R_h is based on values for altered Samail ophiolite [McCulloch, R. Gregory, G. Wasserburg, H. Taylor, *Earth Planet. Sci. Lett.* **46**, 201 (1981)], fluids from Iceland [H. Elderfield and M. Greaves, *Geochim. Cosmochim. Acta* **45**, 2201 (1981)], and epidote from the Troodos ophiolite [B. Smith *et al.*, in *Symposium, Troodos '87: Ophiolites and Oceanic Lithosphere Abstr.* (Geological Survey Department, Nicosia, Cyprus, 1988) p. 162]. The modern $^{87}Sr/^{86}Sr$ ratio of the oceans and the better constrained values for the other fluxes are used to determine the product J_hR_h. A value of 0.705 for R_h corresponds to a J_h of 1.2×10^{10} mol per year. Current estimates of J_h range from 0.3×10^{10} to 1.4×10^{10} mol per year [see M. Delaney and E. Boyle, *Paleoceanography* **3**, 137 (1988)].
29. Dissolution and recrystallization of submarine carbonate sediments provides Sr with $^{87}Sr/^{86}Sr$ ratios mostly between 0.707 and 0.709. The ratio and flux for diagenesis of submarine sediments (R_c = 0.7085, $J_c = 3.0 \times 10^9$ mol per year) are based on studies of pore fluids [H. Elderfield and J. Gieskes, *Nature* **300**, 493 (1982); M. Palmer and H. Elderfield, *ibid.* **314**, 526 (1985)].
30. Based on a seawater Sr concentration of 7.65 ppm [see (*27*)].
31. We thank D. V. Kent, N. J. Shackleton, J. G. Moore, and the Deep Sea Drilling Project for providing samples. The manuscript was improved by comments from B. Stewart and two anonymous reviewers. An earlier version was reviewed by G. Bebout, F. Richter, and R. Shreve. This work was supported by donors of the Petroleum Research Fund, administered by the American Chemical Society, by National Science Foundation grants EAR 85-07995, EAR87-20609, and EAR88-04609 and by the director, Office of Energy Research, Office of Basic Energy Sciences, Engineering and Geosciences Division of the U.S. Department of Energy under contract No. DE-AC03-76SF00098.

1 February 1990; accepted 1 May 1990

Synchronous, Alternating, and Phase-Locked Stridulation by a Tropical Katydid

ENRICO SISMONDO

In the field the chirps of neighboring *Mecopoda* sp. (Orthoptera, Tettigoniidae, and Mecopodinae) males are normally synchronized, but between more distant individuals the chirps are either synchronous or regularly alternating. The phase response to single-stimulus chirps depends on both the phase and the intensity of the stimulus. Iteration of the Poincaré map of the phase response predicts a variety of phase-locked synchronization regimes, including period-doubling bifurcations, in close agreement with experimental observations. The versatile acoustic behavior of *Mecopoda* encompasses most of the phenomena found in other synchronizing insects and thus provides a general model of insect synchronization behavior.

INSECTS OF SEVERAL ORDERS PRODUCE rhythmic signals that are synchronous or regularly alternating with those of conspecific individuals. Notable examples are the songs of the cricket *Oecanthus* (*1*), the katydids *Pterophylla* (*2*), *Pholidoptera* (*3*), and *Ephippiger* (*4*), and the cicada *Magicicada* (*5*), as well as the flashing of the tropical fireflies *Pteroptyx* (*6, 7*). These phenomena have been explained in terms of inhibition-excitation (*3*), two proepisodic mechanisms (in which the stimulus precedes the chirp) (*1*), anticipatory versus paced synchronization (*6*), and the resetting of an internal pacemaker (*7*). I report an analysis of the song of *Mecopoda* species S (*8*): its acoustic behavior is analyzed in terms of the phase-response curve (PRC) and explored by iteration of the Poincaré map (*9*) and by numerical simulation of the interaction of two individuals.

The song of *Mecopoda* S consists of chirps (*10*) emitted every 1.5 to 3 s (Fig. 1, A and B): the chirp rate (CR) is temperature-dependent (Fig. 1C) in a manner consistent with that of other tettigoniids (*11*). In free run (without external stimulus), the period between the onset of successive chirps varies about the mean with a standard deviation in the range 35 to 45 ms (Fig. 1E) (*12*). The average CR in free run drifts with time (Fig. 1F). After entrainment to short-period stimuli, recovery to the free-run CR is slower than recovery time from long-period entrainment; to compensate for these effects, I used an empirical model to predict the "adapted" unconstrained period in simulation work (Fig. 1D). In the field, groups of males synchronize their chirps. Pairs separated by more than 3 to 4 m sometimes alternate chirps instead, each with a longer period than when synchronizing.

I generated artificial signals used for entrainment by computer-controlled playback of a digitized genuine chirp at controllable rate and intensity. Both stimulus and response chirps were recorded on separate tape channels; I then scanned the tape at 960 samples per second per channel to detect and record the onset of each chirp (*13*). Playback of a single isolated pulse from the stimulus chirp elicited normal response, with a minimum latency of 75 ± 9 ms; this length of time is much shorter than the duration of a complete chirp, justifying the use of stimulus onset as the analytical variable.

I obtained PRCs for 15 individuals,

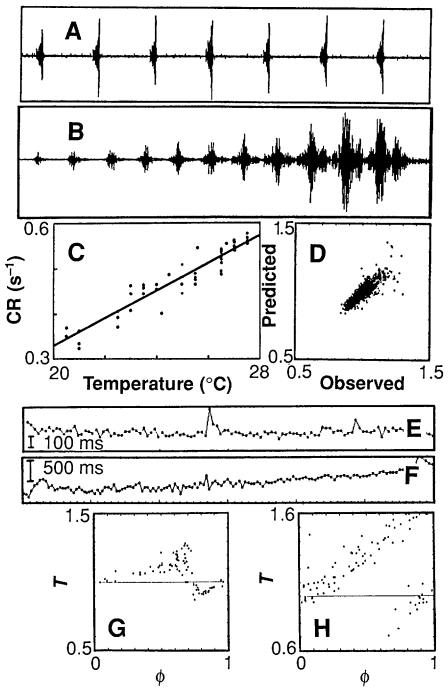

Fig. 1. (**A**) *Mecopoda* species S: A 12.6-s oscillogram of a series of chirps. (**B**) A 227-ms oscillogram of a typical single chirp. (**C**) Temperature dependence of CR (pooled data for three individuals and linear least-squares fit). (**D**) Empirical model of period adaptation function, predicted versus observed free period (normalized to T_0) after various entrainment episodes. (**E**) A 200-s free run showing cycle-to-cycle variation in chirp period. (**F**) A 240-s free run showing long-term drift in chirp period. (**G**) Atypical type I PRC (different individual from that shown in Fig. 2). (**H**) *Mecopoda* species N: PRC at 0 dB and 2.9 m.

22 Leedon Road, Singapore 1026, Republic of Singapore.

whenever possible at more than one stimulus intensity (*14*). The procedure that gave the most reproducible results involves single-chirp, random-phase perturbation of the free-run song every 8 to 12 natural chirps: under these conditions there is no interference from adaptation effects.

The intrinsic period T_0 was taken as the mean of the last three prior unperturbed periods, thus compensating for any long-term drift in the CR. Defining the onset of the last undisturbed chirp as $t(0)$, of the stimulus as $t(s)$, and of the next chirp as $t(p)$, the phase ϕ is

$$\phi = [(t(s) - t(0)]/T_0 \quad (1)$$

and the normalized perturbed period is

$$T = [t(p) - t(0)]/T_0 \quad (2)$$

A plot of T versus ϕ yields the PRCs shown in Figs. 1G and 2, A and D (*14*). The PRC has two branches, with a slope near unity at high stimulus intensities and a slope that approaches the horizontal as stimulus intensity goes to zero. Normally the PRC is of type 0 (Fig. 2A) with a clear discontinuity at phase ϕ_d near 0.65 to 0.75, where the branches typically overlap slightly along the phase dimension. Most specimens retain a type 0 PRC down to very low stimulus intensities; rare individuals do make the transition to type I PRC as stimulus intensity is reduced, and one showed type I PRC under all conditions (Fig. 1G).

I carried out synchronization runs at varying stimulus periods from 500 ms to 6 s. During a run, I varied the entraining period periodically up or down without interruption in steps of 25 or 50 ms, thus minimizing phase shifts and unpredictable adaptation effects (abrupt CR changes frequently cause the insect to stop singing altogether). Analysis of the runs indicates that the insect is capable of stable phase-locked response in the range from 5:1 (one beat for every five stimulus beats) to at least 1:2 (two chirps for every stimulus) (Figs. 2, B and E, and 3A). Near the extremes of the 1:1 range, transient phase-locks of the type $n:(n + 1)$ and $n:(n - 1)$ occur, where n can be quite large (>15). The range of stimulus rates for each phase-locked regime is wider at high stimulus intensity. Hysteresis effects are important (*15*): both the range and the stability of each mode are affected by whether the range is approached from a higher or a lower stimulus CR.

Iteration of the Poincaré map (*9*) for different values of the normalized stimulus period produced the rate-phase plots of Fig. 2, C and F, showing the locus of phase in successive response intervals as a function of normalized stimulus period. Analysis of these plots and numerical simulation reveal the existence of discrete phase-locked regions corresponding to different stimulus rate ranges: these are plotted in Fig. 2, B and E. The predicted position and width of phase-locked regimes are in reasonably good agreement with observation. Some iterated maps show the presence of period-doubling bifurcations at the extremes of the 1:1 range (*16*), and a few unmistakable instances of period-doubling are observed experimentally (Fig. 3B).

I recorded duets of synchronization and alternation between eight pairs of individuals and analyzed them using the same techniques as above. Figure 3, C through F, shows representative results. If two synchronizing individuals have roughly the same intrinsic CR, the lead changes periodically between them (Fig. 3C); mean lead lag is of the order of 39 ± 25 ms, shorter than the minimum latency for response to isolated chirps. The joint CR is irregular and the average entrained period is shorter (typically by 50 to 200 ms) than that of each individual in free run under the same conditions. This result arises from the asymmetry in slope of the PRC in the neighborhood of $\phi = 1$: the lagging individual, stimulated with $\phi < 1$ (lower branch of the PRC), experiences a period shortening greater than the period lengthening of the leading individual (stimulated with $\phi > 0$); the consequent period contraction is preserved by the long-term adaptation phenomenon, which is biased to favor shorter periods. This phenomenon is the basis for "anticipatory synchrony" (*6*).

If one individual's song is naturally faster than the other, he leads most cycles and his CR is more uniform than that of the lagging individual (Fig. 3D). Under natural conditions one occasionally finds phase-locked regimes of the $n:(n + 1)$ type, in the range 6:7 to 3:4, most commonly 4:5 (Fig. 3E); I once recorded 2:2 response, in which one of the males made alternating loud and faint chirps, passing to 2:1 response as the faint chirps became inaudible. Experimental chilling of one of the two individuals slowed his CR (Fig. 1C) and resulted in 5:6 or 4:5 regimes, rapidly passing to stable 1:2 phase-locked synchronization.

It was also possible to use the model designed to iterate the Poincaré map in simulating mutual interaction by utilizing it for both stimulus and response. With different combinations of PRCs and values of T_0 to represent pairs of individuals, the model predicts a small number of stable phase-locked regimes: 1:1 (synchronous or alternating), 5:6, 4:5, 3:4, 2:3, and 1:2; in actual duets I have observed all of these except the 2:3 mode.

Analysis based on the reciprocal effect on each other's PRC yields the conditions for stable alternation (Fig. 3F): obviously the periods of both specimens must be equal, and the phase ϕ for each one must intersect his PRC at the perturbed period T. If we assume for simplicity that the PRCs and the intrinsic periods T_0 are equal for both individuals and that stochastic noise in CR is zero, then the stable alternation point (ϕ_a, T) is such that

$$T = f(\phi_a) = 2\,\phi_a \quad (3)$$

If the upper branch of the PRC is too steep (or too short) to satisfy Eq. 3 at any point,

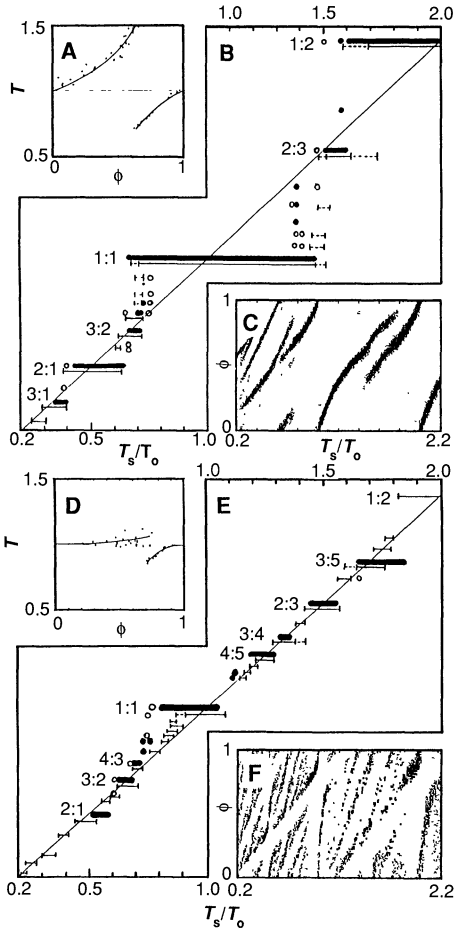

Fig. 2. Periodic stimulation at 0 dB and a distance of 2.9 m. (**A**) Phase response curve: original data and analytical representation. (**B**) Plot of Cantor function showing phase-locked modes in entrainment to artificial stimuli. Heavy lines and filled circles, observed stable phase-locked ranges; open circles, observed short-lived unstable phase locks; fine lines, ranges predicted by iteration of the Poincaré map: the dotted segments mark unstable or transient regions. (**C**) Rate-phase plot obtained by iteration of the Poincaré map (50 iterations at each stimulus rate); note relatively few but well-defined phase-locked regions. (**D–F**) Same individual and distance, stimulus at −25 dB. Note the multiplicity of ill-defined phase-locked regions; most have narrow ranges and not all were observed experimentally.

alternation is impossible. If the PRC contains a point satisfying Eq. 3 and a chirp occurs with phase ϕ in the range

$$[f(\phi) - \phi_d] < \phi < \phi_d \quad (4)$$

then on successive cycles ϕ converges on ϕ_a and alternation becomes established. The presence of stochastic noise reduces the width of the actual stability range compared to that of the theoretical stability range. Realistic situations, in which noise is present and the PRCs and T_0 are different, need not satisfy Eq. 3: they are best analyzed by numerical simulation, which, in the simplest case, confirms the above conclusions.

These results explain why males of *Mecopoda* S always synchronize when they are in close proximity and only alternate when they are at greater distances from each other.

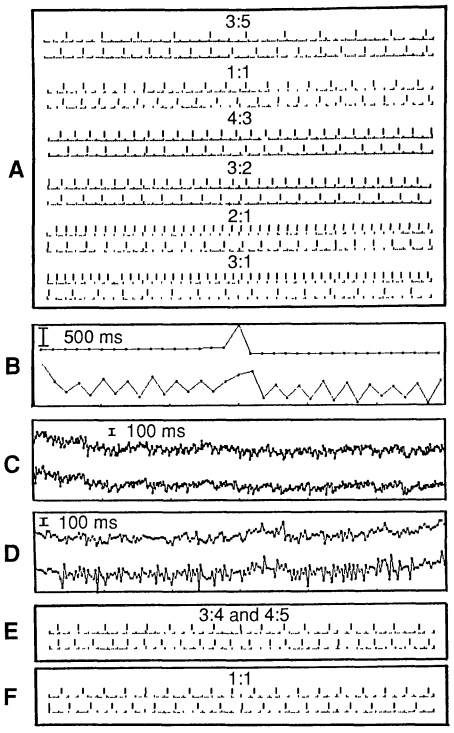

Fig. 3. Entrainment to artificial and natural stimuli. (**A**) Representative 40-s examples of phase-locked synchronization to artificial stimuli; the event markers represent the onset of stimulus (above) and response (below). The average response CR for the first five records is similar, but the chirp intervals are grouped in patterns that repeat every n cycles, where $m:n$ is the phase-locked ratio: especially evident in the 3:5 and the 4:3 examples. (**B**) Period-doubling bifurcation (below) in entrainment to uniform artificial stimulus (above). (**C**) A 10-min record of 1:1 synchronization by two individuals with similar chirp rates: upper individual leads 210 times, lower individual 202 times. (**D**) An 8-min record of 1:1 synchronization by two individuals with different natural CRs: upper individual leads 176 times, lower individual 29 times. (**E**) A 40-s sample of natural 3:4 and 4:5 synchronization between two males, both at 27°C. (**F**) A 40-s sample of natural stable alternation between the same two individuals.

At separations of less than about 3 m, the mutual stimulus is loud, giving steep PRCs that fail to meet the conditions for stable alternation: synchrony is the only possible regime. At slightly greater distance, the PRCs meet the conditions for alternation but the stability range is narrow: stochastic noise will sooner or later force the operating point outside the stable range and lead to in-phase synchrony. Stable long-term alternation is only obtained with separations greater than 4 to 5 m.

Many of the reported modes of synchronization in insect communication are within the versatile repertoire of *Mecopoda* S. The data reported for *Oecanthus fultoni* Walker are amenable to the type of analysis presented here. In particular, the existence of 2:1 phase locks and the observation that, when the cricket synchronizes with an artificial signal (*1*, p. 893), "the cricket fails to improve its phase relations with a faster or slower broadcast signal that it is equaling in chirp rate" (as in Fig. 3A, 1:1) is predictable from the phase resetting data shown in (*1*).

The two branches of the PRC represent the two "proepisodic mechanisms" postulated to explain *O. fultoni*'s performance. The data presented for *Pholidoptera griseoaptera* (DeGeer) (*3*), viewed in the light of the present work, suggest that "inhibition" and "excitation" proposed to explain its alternating and synchronous behavior are two facets of a more general mechanism amenable to phase-response analysis. The concept of "anticipatory synchrony" invoked for the flashing of *Pteroptyx malaccae* (*6*) is based on the observation that the time difference between the signals of synchronizing individuals is shorter than the response latency to an external signal: the same is observed in *Mecopoda* S. The entrained period of synchronizing pairs of *Mecopoda* S is shorter than the free-run period of either individual, a phenomenon also reported for the flashing of *Pteroptyx cribellata* (*7*). In both cases, mutual interaction is not simply response to a "pacesetter" individual but involves "anticipatory synchrony."

Mecopoda species N, a sibling species of *Mecopoda* S (*8*), synchronizes but never alternates, and in mutual stimulation the entrained period is shorter than the free-run period. With signals of normal intensity, its PRC has virtually straight branches with high slope (Fig. 1H), similar to the results reported for *O. fultoni* (*1*): any phase change in the entrainment signal causes an immediate phase adjustment in the response of nearly the correct magnitude to reestablish synchrony by the next chirp or two. This situation is easily represented by a single resettable oscillator and may be viewed as the limiting case for *Mecopoda*. Stridulation

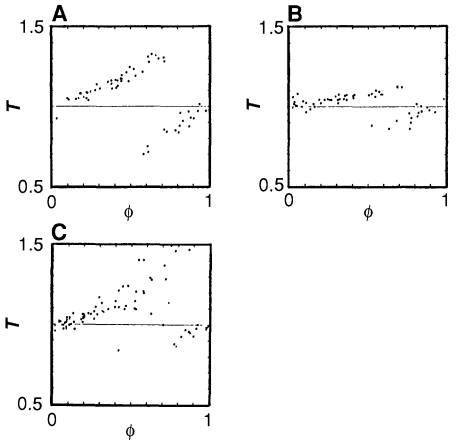

Fig. 4. Simulated PRCs produced by periodic stimulation of the multiple-oscillator model described in the text: (**A**) 100 elementary oscillators, stimulus amplitude = 100 (arbitrary units); (**B**) 100 elements, stimulus amplitude = 50; (**C**) 20 elements, stimulus amplitude = 100.

in *Mecopoda* N is also closely analogous to the flashing of *Pteroptyx cribellata*, for which a resettable relaxation oscillator model was originally proposed (*7*); however, with low-intensity stimuli the PRC of *Mecopoda* N approaches the shape of that for species S and can no longer be represented by such an elementary model. It would be instructive to study the response of *Pteroptyx* to very low-level light signals, to determine whether it deviates from normal behavior in a similar fashion.

Because the PRC proves to be a powerful predictor of the synchronization behavior of *Mecopoda*, it is important that any model of its internal oscillator-trigger system be capable of reproducing the free-run characteristics as well as the slope and curvature of the PRC under a variety of conditions; a simple resettable oscillator such as that proposed for *Pteroptyx* (*7*) is not adequate for the task. I programmed a hypothetical model consisting of a population of free-running elementary relaxation oscillators (EROs), whose intrinsic periods have a Gaussian distribution; a summing element accumulates the number of ERO firings, triggering a chirp and resetting the accumulator when that number reaches a predetermined threshold expressed as a fraction of the total number of EROs. An external stimulus decrements the accumulator in proportion to stimulus intensity if the current sum is less than a critical fraction ("inhibition") but increments the accumulator (lowers the threshold, "excitation") if the current sum is higher. With one-time tuning of only four parameters to define the oscillator system, the model yields realistic type 0 PRCs under periodic stimulation over a range of stimulus intensities; with 100 EROs the fit to actual

PRCs is very good (Fig. 4, A and B), but simulation with as few as 20 elements yields credible results (Fig. 4C). The model predicts the shape and slope of the PRC, the effect of stimulus intensity, the overlap of branches at the discontinuity, and the stochastic noise in free run but does not predict the long-term drift and adaptation phenomena. Simulation runs based on the use of this oscillator model instead of the analytical representation of the PRC yield the expected synchronous and alternating 1:1 modes as well as the usual $n:(n + 1)$ and $m:n$ phase locks. I make no claim for the "truth" of the model, which is introduced only to show that a simple mechanistic explanation with a minimum of ad hoc assumptions can account for the versatile synchronization behavior of *Mecopoda*.

REFERENCES AND NOTES

1. T. J. Walker, *Science* **166**, 891 (1969).
2. B. B. Fulton, *J. Elisha Mitchell Sci. Soc.* **50**, 263 (1934).
3. M. D. R. Jones, *Nature* **203**, 322 (1964); *J. Exp. Biol.* **45**, 15 (1966); *ibid.*, p. 31.
4. R. G. Busnel, M. C. Busnel, B. Dumortier, *Ann. Epiphyt.* **3**, 451 (1956); R. G. Busnel, B. Dumortier, M. C. Busnel, *Bull. Biol. Fr. Belg.* **90**, 219 (1956).
5. R. D. Alexander, in *Animal Sounds and Communication*, W. E. Lanyon and W. N. Tavolga, Eds. (American Institute of Biological Sciences, Washington, DC, 1960).
6. J. Buck and E. Buck, *Science* **159**, 1319 (1968).
7. F. E. Hanson, J. F. Case, E. Buck, J. Buck, *ibid.* **174**, 161 (1971).
8. In southeast Asia there are several sibling species of *Mecopoda*, loosely referred to *M. elongata* (L.): morphologically they are very similar, but their songs and geographic distribution are diagnostic. I am provisionally using code letters to identify them: species S is found in the lowlands of peninsular Malaysia and is the common species in Singapore; at 25°C it chirps every 2.1 s, and each chirp consists of 8 to 13 pulses (wing strokes). Species N is from Bali, Indonesia: it sings at a rate of 4.5 chirps per second at 25°C, and each chirp consists of 4 to 5 pulses. Voucher specimens and tape recordings of these two and two additional species have been deposited in the British Museum (Natural History).
9. The Poincaré map is defined by

$$\phi(i + 1) = 1 - f[\phi(i)] + \phi(i) + T_s/T_0 \pmod 1$$

where T_s is the stimulus period and $f[\phi(i)]$ is the perturbed cycle length T given by the PRC (*14, 16*). The branches of the PRC were fitted with simple polynomial functions and, at each stage in the iteration of the Poincaré map, superimposed with random noise of magnitude appropriate to the particular insect; the intrinsic period T_0 at each iteration was corrected by the empirical adaptation function discussed above.
10. Technically these are "echemes" in the terminology of W. B. Broughton [*Physiol. Entomol.* **1**, 103 (1976)]; "chirp" is easier to use, and in this case, closely onomatopoeic.
11. Extrapolation of the linear least-squares fit to the data from three individuals yields a temperature of 9.2°C at zero CR. This is near the mean of the range reported by T. J. Walker, *J. Comp. Physiol.* **101**, 57 (1975).
12. If I use precisely timed, computer-generated chirps previously recorded on tape, the overall system error in detecting chirp onsets is about 2 ms; with natural song the first pulse of some chirps may be missed, which introduces an error of about 25 ms equivalent to 1 to 2% of the chirp period.
13. *Mecopoda* males were kept in screen cages on food plants and misted with water daily. Captive adults lived as long as 4 months: the characteristics of stridulation became established about 10 days after molting and remained unaltered thereafter. Temperature ranged from 24° to 30°C and was recorded with each run. Runs were taped on a Sony TC-D5M with two Audio Technica AT-811 microphones. Stimulus generation, data acquisition, and analysis were carried out on an XT-compatible computer fitted with a 12-bit analog-to-digital and digital-to-analog interface. Stimulus signals were amplified and played back through a piezoelectric tweeter. Oscillographic and fast Fourier transform spectral analysis of the artificial chirp showed it to be virtually indistinguishable from the original. A signal volume equal to that of the natural chirp was taken as the 0-dB [sound pressure level (SPL)] reference; SPL levels for signals at other volumes were calculated from relative oscillographic amplitude.
14. For general discussion of phase response (or resetting) curves, see L. Glass and M. C. Mackey, *From Clocks to Chaos* (Princeton Univ. Press, Princeton, NJ, 1988). See also T. Pavlidis, *Biological Oscillators: Their Mathematical Analysis* (Academic Press, New York, 1973). For a classical example, see D. S. Saunders, *J. Comp. Physiol.* **124**, 75 (1978).
15. Hysteresis of this type is also present in purely physical systems: see J. P. Gollub, T. O. Brunner, B. G. Danly, *Science* **200**, 48 (1978).
16. If the maps are iterated without superimposed simulated noise, some of them yield classical period-doubling cascades and chaotic regions. The presence of noise obliterates most of these phenomena, but bifurcations are sometimes discernible. See L. P. Kadanoff, in *Regular and Chaotic Motions in Dynamic Systems*, G. Velo and A. S. Wightman, Eds. (North Atlantic Treaty Organization Advanced Science Institutes, Series B, Plenum, New York, 1985), p. 118; R. M. May, *Science* **186**, 645 (1974); M. R. Guevara, L. Glass, A. Shrier, *ibid.* **214**, 1350 (1981).

17. I thank D. R. Ragge of the British Museum (Natural History) for helpful suggestions and advice on the taxonomy of *Mecopoda*.

24 January 1990; accepted 25 April 1990

The Role of Ocular Muscle Proprioception in Visual Localization of Targets

GABRIEL M. GAUTHIER, DANIELLE NOMMAY, JEAN-LOUIS VERCHER

The role of ocular muscle proprioception in the localization of visual targets has been investigated in normal humans by deviating one eye to create an experimental strabismus. The passively deviated eye was covered and the other eye viewed the target. With a hand-pointing task, targets were systematically mislocalized in the direction of the deviated nonviewing eye. A 4- to 6-degree error resulted when the nonviewing eye was offset 30 degrees from straight ahead. When the eye was deviated, the perceived "straight-ahead" was also displaced, by a similar amount, in the same direction. Since the efferent motor commands to the displaced and to the nondisplaced eyes are presumably identical by the law of equal innervation, the mislocalization of visual objects must be attributed to the change in proprioceptive information issued from the nonviewing, deviated eye. Thus proprioception contributes to the localization of objects in space.

IN ORDER TO LOCALIZE AN OBJECT IN space, when the head is fixed, the central nervous system (CNS) must use a combination of visual (retinal) information and a knowledge of the position of the eye in orbit. Two major hypotheses have been put forward to explain how eye position is sensed: the outflow or efference copy hypothesis, first suggested by Von Helmholtz in 1867 (*1*), which is based on sensing the motor commands to the ocular muscles, and the inflow or afferent hypothesis, first suggested by Sherrington in 1918 (*2*), which is based on sensing proprioceptive inputs from the ocular muscles themselves.

Until recently, the efferent copy hypothesis has been accepted as the correct mechanism for visual target localization. No certain function was attributed to ocular muscle proprioception. But recent anatomical studies confirm widespread projections of orbital muscular afferents to a variety of CNS structures concerned with the control of movements of the eyes and of the head (*2*). Physiological studies, too, suggest a role for proprioception in various visual functions, such as development of the orientation of receptive fields (*3*). Finally, studies in humans with naturally occurring strabismus give hints of a functional role for proprioception in the localization of visual targets. We have found that some strabismics (*4*), either eso- or exo-deviated, when tested in a hand-pointing task, make errors as large as 10° to 20° in the direction of the nonfixing eye.

From these observations, we hypothesized that the visual localization mechanism relies on both afferent and efferent information derived from both eyes, whether or not both eyes are used to fixate the target. To test this hypothesis we deviated the non-

Laboratoire de Contrôles Sensorimoteurs, Département de Psychophysiologie, Unité Associée CNRS 372, Université de Provence, Avenue Escadrille-Normandie Niemen, 13397 Marseille cedex 13, France.